# Liver Anatomy and Cross-Sectional Imaging Techniques: A Practical Approach

Parul Samir Garde[1] Rahul Bhagwan Bhute[2]

[1] Department of Radiology and Imaging, Global Hospitals, Mumbai, India
[2] Department of Radiology and Imaging, King Edward Memorial Hospital Parel, Mumbai, India

**Address for correspondence** Parul Samir Garde, DMRD, DNB, Department of Radiology and Imaging, Global Hospitals, Mumbai 400012, India (e-mail: parulsamir@gmail.com).

J Gastrointestinal Abdominal Radiol ISGAR 2023;6:89–100.

**Abstract**

In the past decade or two, there has been a significant change in the epidemiology of liver diseases, such as rise in the incidence of nonalcoholic steatohepatitis, good control of viral load in hepatitis B and C related liver diseases, and revolutionary changes in the treatment of hepatocellular carcinoma. Hence, monitoring of these diseases warrants effective noninvasive imaging techniques. Besides, organ transplantation has evolved to play a major role in the treatment of chronic liver diseases and acute liver failures. With the advent of better technology and new imaging sequences in cross-sectional imaging, there has been a dramatic change in the arena of liver imaging. Knowledge of these imaging modalities and effective application of the existing and new imaging techniques is essential to meet these changing clinical needs. This article aims at revisiting the liver anatomy from a practical stand point and touches upon the key cross-sectional imaging techniques of computed tomography and magnetic resonance imaging with recent advances.

**Keywords**
- anatomy
- cross sectional
- imaging
- liver

## Introduction

Epidemiological changes in the lifestyle over past two decades have led to an increase in the incidence of nonalcoholic fatty liver disease and in turn chronic liver parenchymal disease. Besides, there have been significant changes in the treatment of viral hepatitis C. Similarly, a variety of treatment options are now available for hepatocellular carcinoma (HCC) ranging from targeted drug therapy, immune modulation therapy, locoregional treatment, and radiation therapy. These have led to the development of several noninvasive tools for monitoring the progress of liver parenchymal disease and its response to medical management.

On the other hand, organ transplantation has proved to be a game changer in the treatment of decompensated liver diseases and chronic liver diseases with HCC (within operable criteria). Hence, thorough knowledge of hepatic segmental, vascular, and biliary anatomy is the need of the hour to guide in the process of live donor liver transplantation and surgical resection of liver tumors.

Major technological advances have revolutionized cross-sectional imaging, thus providing a new perspective to liver imaging and catering to all these varied causes.

This article aims at the following:

- Revisiting the cross-sectional liver segmental, vascular, and biliary anatomy, with practical guide points from the perspective of surgical resection and transplantation.
- Use of the right cross-sectional imaging technique for the liver in a unit equipped with a basic multidetector row computed tomography (CT) and 1.5-T magnetic resonance imaging (MRI), so as to get the best results from available resources. It is based on the guidelines laid down by liver imaging reporting and data system (LI-RADS v2018).[1]

**article published online**
April 17, 2023

**DOI** https://doi.org/10.1055/s-0043-1767727.
**ISSN** 2581-9933.



Thieme Medical and Scientific Publishers Pvt. Ltd., A-12, 2nd Floor, Sector 2, Noida-201301 UP, India

## Anatomy of the Liver: from a Clinicoradiological Perspective

### Segmental Anatomy of Liver

Understanding of the lobar and segmental classification of the liver is of immense help in the preoperative evaluation and planning in the treatment of benign and malignant liver tumors. Another application of this knowledge is for living donor liver transplantation in adult and pediatric patients, in which the volume of liver graft and remnant liver volume are of utmost and primary importance for donor selection.

There are multiple systems used for liver segmentation. The most commonly used and accepted standard is the Couinaud system, wherein the liver is divided into eight segments based on three portal scissura (right, middle, and left hepatic veins). This division is based on the orientation of hepatic veins and the level of portal vein bifurcation.[1] Each segment is an independent functional unit having its own function, inflow, and outflow of blood, and biliary and lymphatic drainage.[2] An imaginary line, namely, Cantlie's line, traverses from the gall bladder fossa to the left of the inferior vena cava (IVC) dividing the liver into right and left hemi-livers. Alternatively, the middle portal scissura also divides the liver into two halves.

For practical purposes, to uniformly define and classify surgical hepatectomies, the Committee of the International Hepato-Pancreato-Biliary Association recommended a new terminology for liver segmentation.[3] As per this committee, the first-order division is the right and left hemi-liver. So the right hemi-liver consists of segments V to VIII and the left hemi-liver consists of segments II to IV. Resection of these hemi-livers is termed right or left hepatectomy.

The second-order division is separation of two hemi-livers into the following sections: anterior (segments V and VIII) and posterior (segments VI and VII) sections for the right hemi-liver and medial (segments IVa and IVb) and lateral (segments II and III) sections for the left hemi-liver.

The right hepatic vein divides the right hemi-liver into anterior and posterior sections. Segment V is an anterior segment of the right hemi-liver anterior to the right hepatic vein, below the portal vein bifurcation. Segment VIII is an anterior segment of the right hemi-liver anterior to the right hepatic vein above the portal vein bifurcation. The posterior segment above the portal vein bifurcation and posterior to the right hepatic vein is segment VII and below the portal vein bifurcation is segment VI.

The left medial section is between the middle hepatic vein and the fissure for ligamentum teres. It comprises segments IVa and IVb, above and below the portal vein bifurcation plane, respectively. The left lateral section lies medial to the fissure for the ligamentum teres, with segment II above and segment III below the portal vein bifurcation plane (►**Table 1** and ►**Fig. 1**).

Resection of these sections is sectionectomy. When resection includes the right hemi-liver and adjoining left medial section, it is termed extended right hepatectomy or right trisectionectomy. Similarly, resection of the left lobe and right anterior section is termed extended left hepatectomy or left trisectionectomy. Knowledge of these terminologies is important to provide functional liver remnant on CT, in patients with liver masses.

**Table 1** Segmental anatomy of liver

| Segment | Segment/sector description |
|---|---|
| I | Caudate lobe |
| II | Superior left lateral sector/section |
| III | Inferior left medial sector/inferior left lateral section |
| IVa | Superior left medial sector/section |
| IVb | Inferior left medial sector/section |
| V | Inferior right anterior sector/section |
| VI | Inferior right posterior sector/section |
| VII | Superior right posterior sector/section |
| VIII | Superior right anterior sector/section |

In the third-order division, the sections are classified into many types. Surgical resection of a segment is termed segmentectomy. When it involves two segments, it is termed bisegmentectomy. An optional second-order division based on the portal vein is sectors. The corresponding term for resection of these sectors is sectorectomy. In the right hemi-liver, the anterior and posterior sections are synonymous with the anterior and posterior sectors. In the left hemi-liver, the left medial sectors include segments III and IV and the lateral sector includes only segment II.

The caudate lobe or Couinaud segment I has a unique anatomy and vascular supply/drainage and is not a part of the right or left hemi-liver. The anatomy of this segment is as follows. Anteriorly, it is bounded by the fissure for ligamentum venous, posteriorly by the IVC, and inferiorly by the foramen of Winslow. This segment has an arterial and venous supply usually from the right hepatic artery and the right or both branches of the portal vein, with multiple small veins draining directly into the IVC.[4]

## Vascular Anatomy of Liver

### Porta Hepatis

It is the hilum of the liver through which the portal vein, hepatic artery, common hepatic duct (CHD), nerves, and lymphatics enter the liver.

## Arterial Anatomy of Liver

Preoperative evaluation of hepatic arterial anatomy and variations is important to prevent arterial injury during laparoscopic or open laparotomies for liver surgery. Besides, any minimally invasive surgery is going to offer a limited view of the patient's anatomy, which makes preoperative imaging essential for identification of anatomy and potential variations. For liver transplantation, the variations in the arterial anatomy define single or multiple arterial anastomoses for the graft liver in the recipient.

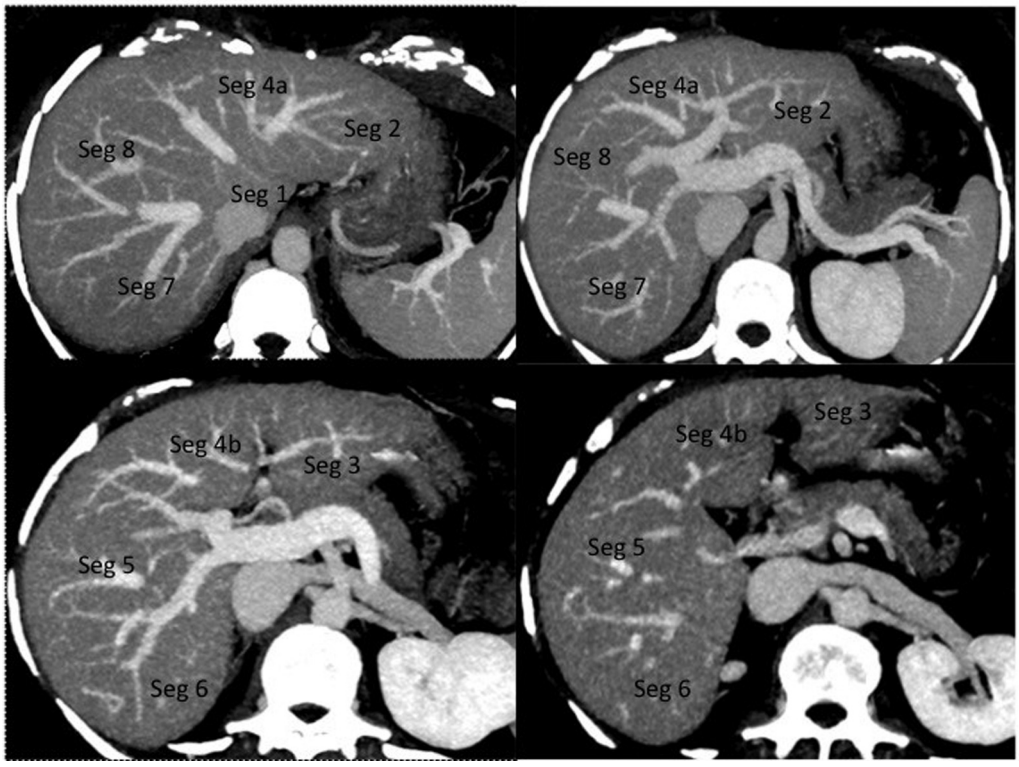


**Fig. 1** Segmental anatomy of the liver on cross-sectional imaging.

Approximately 20 to 25% of blood supply to the liver is by the common hepatic artery (CHA). It is commonly seen as a branch of the celiac trunk. The celiac trunk arises from the abdominal aorta at the D12–L1 vertebral level. After few centimeters of its origin, it commonly trifurcates into the CHA, left gastric artery, and splenic artery. The CHA, after giving off the gastroduodenal artery, continues as the hepatic artery proper, which usually lies anterior to the portal vein and medial to the bile duct. It divides into the right and left branches supplying the respective lobes of the liver. Sometimes the middle hepatic artery may also be present supplying segment IV of the liver. Variations in the hepatic artery are seen in 20% of cases.[5] Common variations in the anatomy of the hepatic artery are given by the Michel classification system (►**Table 2**, ►**Fig. 2**). Hiatt further modified the Michel classification system and added another variation of secluded origin of the CHA from the abdominal aorta.[6]

**Table 2** Michel's classification system of hepatic arterial variations

| Type | Variation |
|---|---|
| I | Hepatic artery from the CHA |
| II | Replaced the LHA from the LGA |
| III | Replaced the RHA from the SMA |
| IV | Replaced the RHA and LHA |
| V | Accessory LHA from the LGA |
| VI | Accessory RHA from the SMA |
| VII | Accessory RHA and LHA |
| VIII | Replaced the RHA and the accessory LHA |
| IX | Replaced the LHA and the accessory RHA |
| X | Entire hepatic trunk from SMA |

Abbreviations: CHA, common hepatic artery; LGA, left gastric artery; LHA, left hepatic artery; RHA, right hepatic artery; SMA, superior mesenteric artery.

## Portal Venous Anatomy

The portal vein is formed by a confluence of the splenic vein and the superior mesenteric vein, posterior to the neck of the pancreas. It travels cranially and to the right in an oblique fashion to the porta hepatis of the liver, where it divides into two branches: right and left. At the level of the porta, the main portal vein lies posterior to the hepatic artery proper and bile duct. The right portal vein has a horizontal course within the liver. It gives off anterior and posterior branches supplying segments V, VIII, and VI, VII. The left branch of the portal vein has an oblique cranial course in the left hemiliver, supplying segments II to IV. A normal portal venous anatomy is seen in 60 to 80% of the population at CT angiography.[7,8] Multiple variations exist; Cheng classified them into four common types (►**Table 3**, ►**Fig. 3**).

Another type is the segment IV branch coming off as a separate branch of the right portal vein.

Practical implication of this anatomy is for planning of liver resections and in pretransplant evaluation of liver donors. When there is crossover of the portal venous supply, that is, segmental portal veins of the right lobe from the left portal vein and the segment IV portal branch from the right

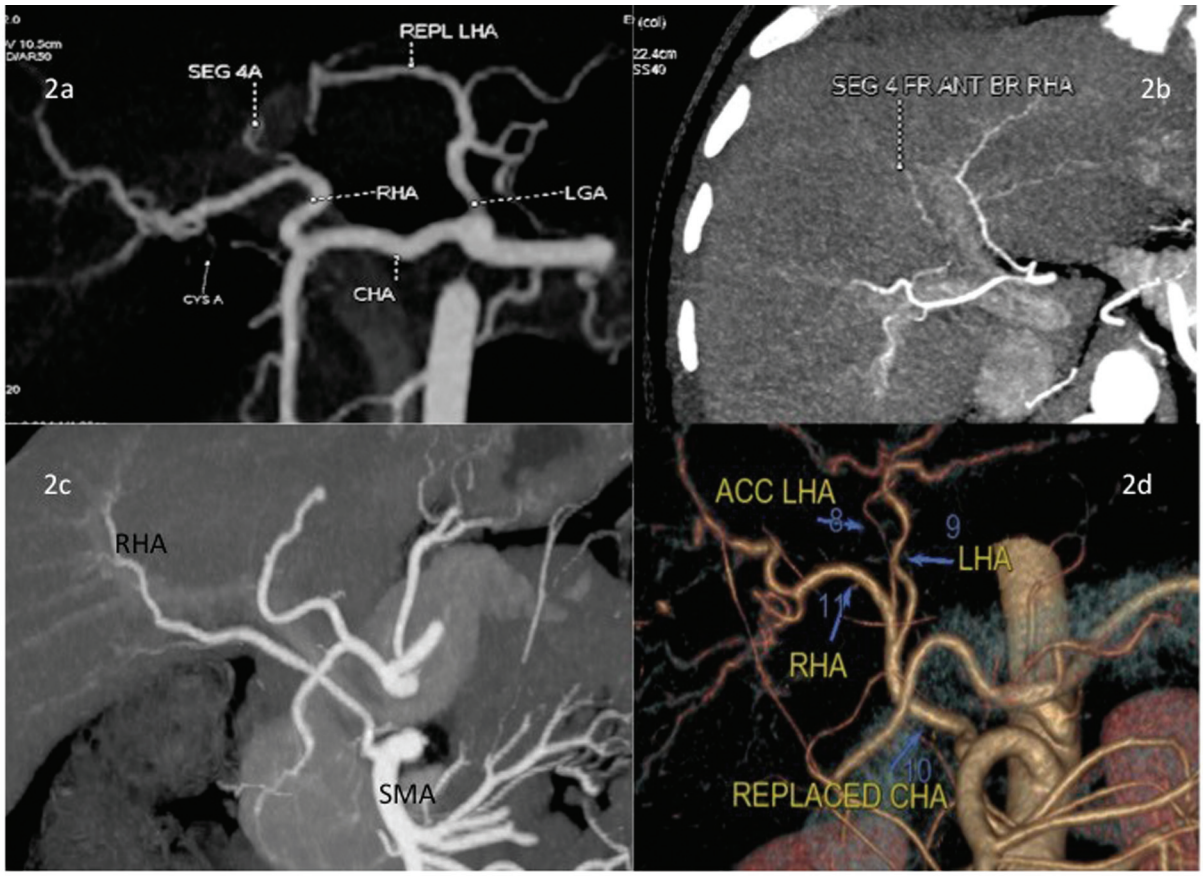


**Fig. 2** Maximum intensity projection (MIP) and volume-rendered images of computed tomography (CT) angiography showing the hepatic arterial anatomical variants. (a) Replaced left hepatic artery arising from LGA. (b) Segment 4 branch arising from RHA. (c) Replaced right hepatic artery arising from SMA. (d) Replaced CHA arising from SMA.

**Table 3** Cheng's classification of variations in portal venous anatomy

| Cheng type | Description |
|---|---|
| I | Normal anatomy with bifurcation into the right and left branches |
| II | Trifurcation pattern, wherein the right anterior and posterior sectoral veins join the left portal vein at the same level |
| III | Right posterior sectoral vein directly arising from portal vein and at a lower level in the hepatic hilum |
| IV | Right anterior sectoral vein arising from the left portal vein |

portal vein, the donor liver anatomy is unacceptable for donation.

### Hepatic Venous Anatomy

Normally, there are three hepatic veins draining into the IVC. The left hepatic vein lies in the left portal scissura and drains segments II and III. The middle hepatic vein lies in the middle portal scissura and drains segment IV, most of the times. It also receives the branches from segments V and VIII.[9] The right hepatic vein is the largest and drains segments V to VIII most times. Single or multiple separate venous channels drain the caudate lobe, directly into the IVC. The middle and left hepatic veins join to form a common trunk in 60 to 95% of cases.[10–12]

Hepatic venous variations are more common in women than in men.[13] A common variant is the presence of the accessory right inferior hepatic vein, which drains into the middle of the retrohepatic IVC.[10] Multiple individual hepatic veins draining separately into the IVC are also seen as a variation (►**Fig. 4**).

The presence of the right inferior hepatic vein and separate veins draining into the IVC implies an increase in the number of venous anastomoses in liver transplant recipients. If the insertion of the accessory vein is close to the right hepatic–IVC confluence, then a common venous channel can be created and single anastomoses with the recipient IVC can be made. Besides accessory hepatic veins with a size of 4 mm or more have to be anastomosed with the recipient IVC to

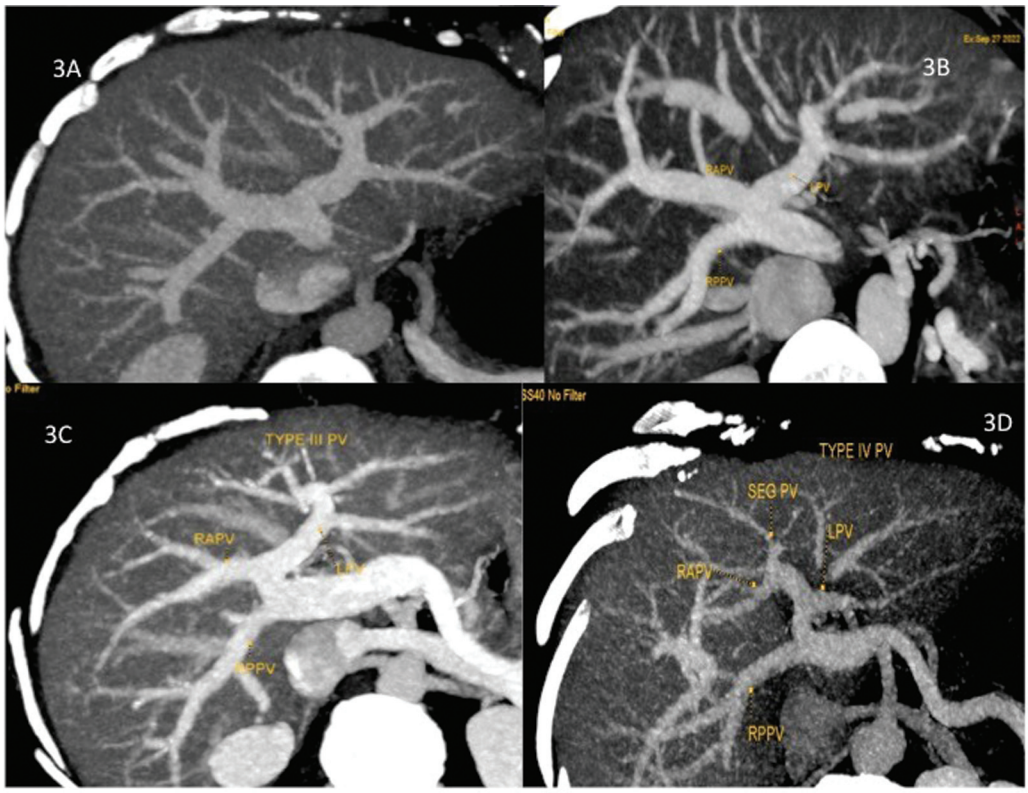


**Fig. 3** Maximum intensity projection (MIP) images on computed tomography (CT) angiography showing variations in the portal venous anatomy. Pictorial depiction of the portal vein variant anatomy. (This image is provided courtesy of Denis Castaing.) (a) Cheng type I portal venous variation. (b) Cheng type II portal venous variation. (c) Cheng type III portal venous variation. (d) Cheng type IV portal venous variation.

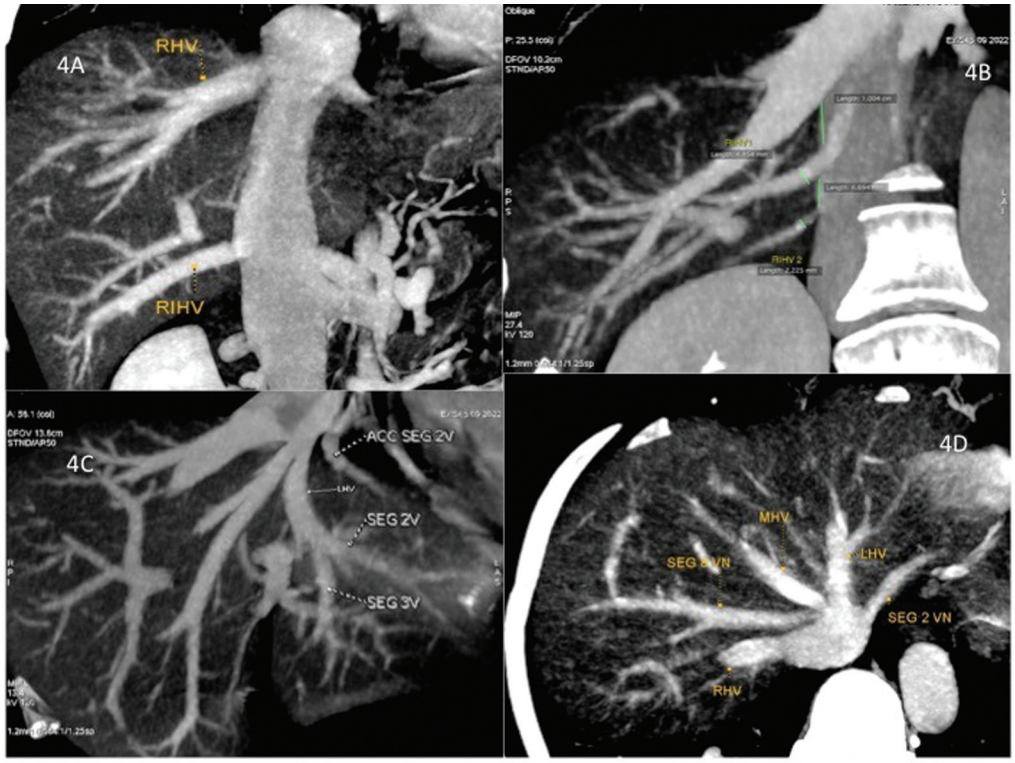


**Fig. 4** Maximum intensity projection (MIP) images of the hepatic venous anatomy variants. (a) Right inferior accessory hepatic vein draining separately into IVC. (b) Two inferior accessory hepatic veins to be labeled separately with individual diameter and distance from RHV-IVC confluence. (c) Accessory segment II hepatic vein draining directly into the IVC- coronal MIP image. (d) Accessory segment II hepatic vein draining directly into the IVC- axial MIP image.

avoid venous congestion in the graft.[10] Thus, information of the size and number of accessory or separate hepatic veins is of practical importance to the transplant surgeon.

### Biliary Anatomy

Bile formed from hepatocytes is drained by the biliary system into the duodenum. The bile ducts are classified into extra- and intrahepatic ducts. Multiple biliary canaliculi from a particular segment join to form segmental bile ducts, which join to form sectional ducts.[14] So the right anterior sectional duct drains segments V and VIII, and the right posterior sectional duct drains segments VI and VII. The left medial sectional duct drains segment IV, and the left lateral sectional duct drains segments II and III. Normally, the right anterior and posterior ducts join to form the right hepatic duct and the left medial and lateral ducts join to form the left hepatic duct. Both the right and left hepatic ducts join to form a CHD.

The cystic duct joins the CHD to form the common bile duct (CBD), which eventually drains into the second part of the duodenum. The cystic duct, CHD, and CBD are extrahepatic ducts.

Practical application of the knowledge of the biliary anatomy is essential for radiologists. Preoperative evaluation of the biliary anatomy prior to laparoscopy and laparotomy for treatment of benign and malignant lesions of the hepatobiliary system is essential. Variations of the biliary system are common occurrence and if not identified on imaging may result in injury with bile leak and peritonitis during liver resection surgeries and in living donor liver transplantations. These may also result in unexpected hepaticojejunal anastomoses in recipients.

The Huang classification of the biliary anatomy is a commonly used system.[15] It is described in ►**Table 4** and ►**Fig. 5**.

Similarly, based on insertion of the segment IV duct onto the left hepatic duct, the right hepatic or sectoral duct, cystic duct, and CHD, variations of the left biliary anatomy have also been described by Huang et al.[15] These variations are classified into B1 to B4 depending on their insertion onto the left hepatic duct, biliary confluence, right hepatic duct, and CHD.

Cystic duct insertion variations are also common, few of the common ones being the following:

- Low insertion into the distal CBD.
- Medial cystic duct insertion.
- Parallel course of the cystic duct with CHD.

## Cross Sectional Imaging of Liver

### Multiphasic Computed Tomography

A good imaging technique is essential in evaluating liver pathology. This is particularly true in a cirrhotic liver, wherein fibrotic, inflammatory, and regenerative changes can alter the hepatic morphology and parenchymal perfusion/outflow, thus reducing conspicuity of the regenerative and dysplastic nodules and, more so, malignant liver masses. This dictum holds true even for evaluation of the anatomy and variants in a prospective liver donor.

It is recommended to include postcontrast late arterial, portal venous, equilibrium phases with unenhanced phase, being optional for complete evaluation of the liver. According to the Liver Imaging Reporting and Data System (LI-RADS), arterial phase hyperenhancement is an important major criterion in the characterization of HCC, without which a lesion cannot be characterized as LI-RADS 5. Lesion de-enhancement on venous phases and enhancing capsule/pseudocapsule also form a part of the major criteria of LI-RADS.

Although the liver CT protocol assessment criteria are not provided by the OPTN or LIRADS guidelines, an important benchmark recommended in the literature is that the liver should be enhanced by a minimum of 50 HU in the portal venous phase. To image the liver in these various blood pool phases, rapid intravenous contrast injection of 4 to 5 mL/s and weight-based contrast dose of 1.5 mL/kg body weight is thus recommended. These form the basis of multiphasic CT imaging of the liver.[1,16,17]

The protocol followed by our institution, in a suspected or known chronic liver disease, is based on the above guidelines and is as given in ►**Table 5**.

The postcontrast phases are obtained at the following time intervals after the start of contrast injection, as described in ►**Table 6**.

**Table 4** Huang's classification of variations in right-sided biliary anatomy

| Huang type | Description |
|---|---|
| A1 | The right posterior duct drains into the right anterior hepatic ducts and joins the left hepatic duct to form the common hepatic duct (CHD) |
| A2 | The right posterior hepatic duct, right anterior hepatic ducts, and left hepatic duct join each other in a trifurcation and form the CHD |
| A3 | The right posterior hepatic duct drains into the left hepatic duct and then joins the right anterior hepatic duct to form the CHD |
| A4 | The right anterior hepatic duct drains into the left hepatic duct and then joins the right posterior hepatic duct to form the CHD (right posterior duct drains into the CHD) |
| A5 | The right anterior hepatic duct drains into the left hepatic duct and forms the CHD. The right posterior hepatic duct drains into the cystic duct |

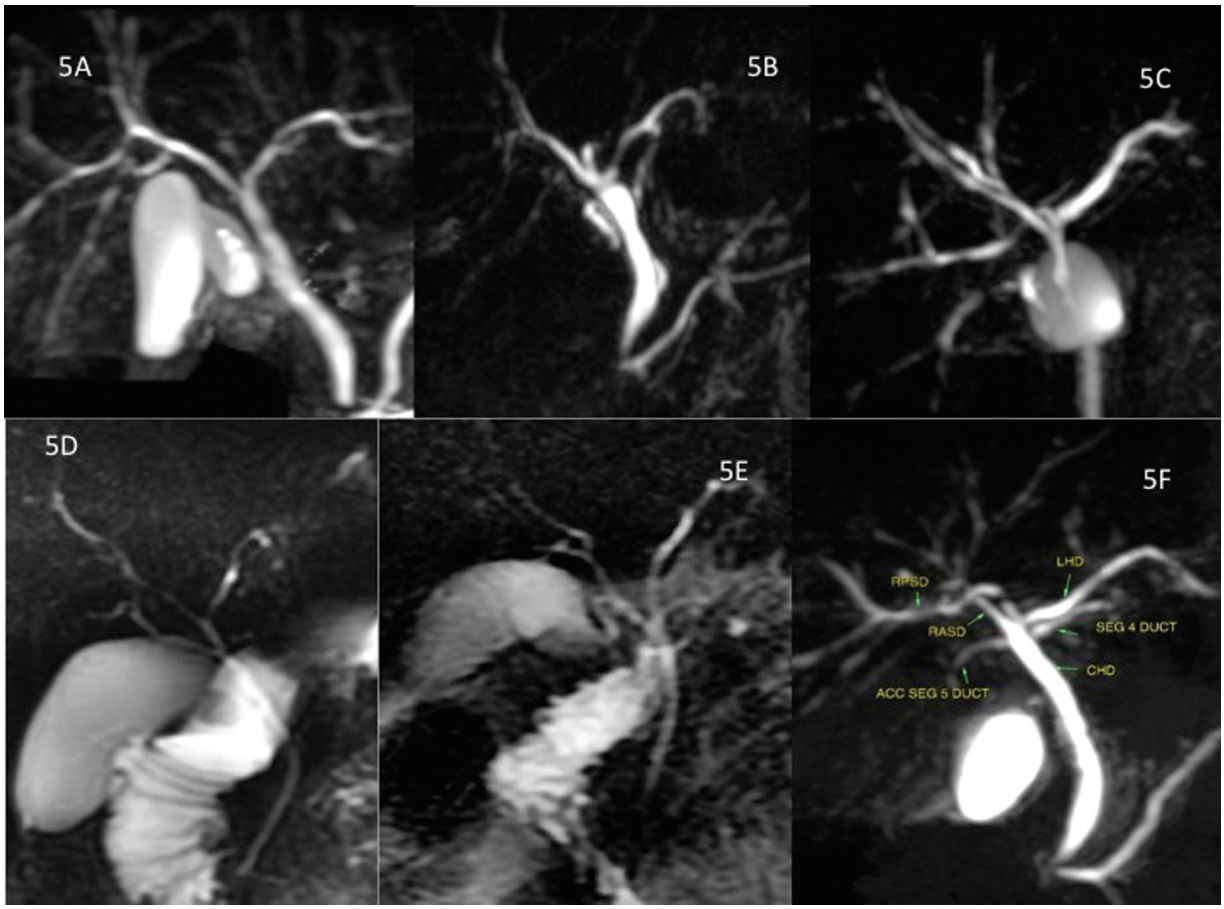


**Fig. 5** Right and left biliary variant anatomy. Maximum intensity projection (MIP) images of 3D magnetic resonance cholangiopancreatography (MRCP). Line diagram to indicate variations in the right biliary anatomy as classified by Huang T.L. (a) A1B1 biliary anatomy. (b) A2B1 biliary anatomy. (c) A3B1 biliary anatomy. (d) A4B1 biliary anatomy. (e) A5B1 biliary anatomy. (f) A3B4 biliary anatomy, with accessory segment 5 duct.

**Table 5** Computed tomography (CT) protocol for multiphasic study for imaging liver

| Scanner | Single-source, dual-energy CT, 64 slices |
|---|---|
| kV (kilovoltage) | 120 |
| mAs (milliamperes) | 350–400 |
| Rotation speed | 0.5 |
| Pitch | 0.984:1 |
| Reconstruction interval | 0.625 mm |
| Threshold | 80 HU |
| Bolus tracking | Region of interest on descending abdominal aorta |
| Concentration of iodine | 370–400 mg% |
| Dose of contrast | 100–120 mL |
| Rate of contrast injection | 4–5 mL/s |

**Table 6** Timings of acquisition (from start of injection) of different postcontrast phases of multiphasic computed tomography (CT) scan of the liver on 64-slice, dual-energy scanner

| | |
|---|---|
| Early arterial phase | 15 s |
| Late arterial phase | 25 s |
| Portal venous phase | 45 s |
| Hepatic venous phase | 60 s |
| Delayed phase | 5 min |

## Importance of Dual-Energy CT

Dual-energy CT (DECT) is based on CT data acquisition at two different energy spectra. It is meant to overcome the shortcoming of contrast-enhanced CT to rely purely on Hounsfield units.[18] Every vendor has adopted a different method of applying this technique for clinical use. These are either prospective or retrospective. Prospective techniques include rotate-rotate technique (Toshiba), dual source and twin beam techniques (Siemens), and rapid kilovoltage peak (kVp) switching (General Electrical). Retrospective techniques include sandwich detector (Philips) and photon counter (Siemens). These are depicted in ►**Fig. 6**.

Rapid kVp switching technique (by General Electrical company) utilizes a single X-ray tube with fast kVp switching with energy separation at the detector level (gemstone scintillator detector). By the virtue of this technique, material decomposition can be done based on the energy-dependent

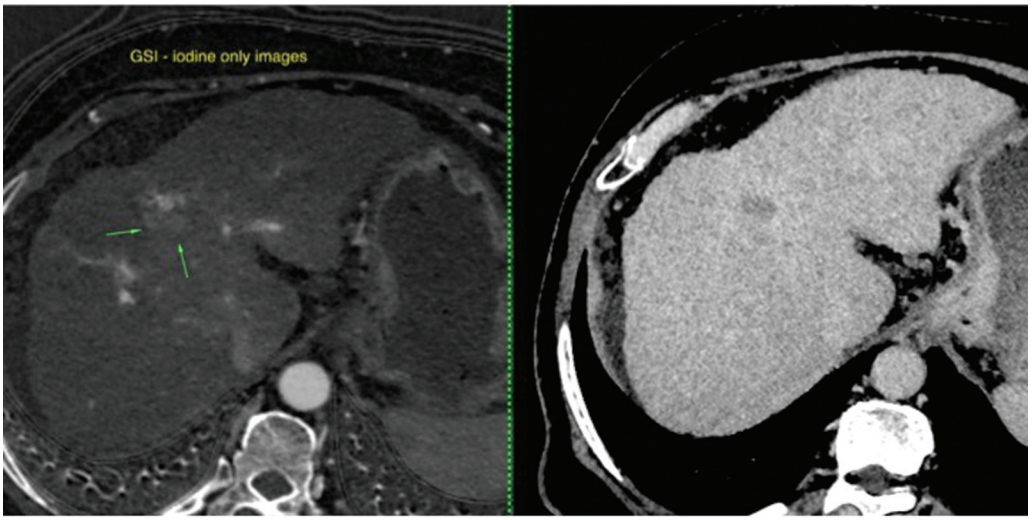


**Fig. 6** Pictorial depiction of dual-energy computed tomography (DECT) scanners and their principle techniques. Axial CT section of the liver in the gemstone scintillator detector (GSI) mode with iodine–water mapping.

attenuation profile of specific materials.[19] Post acquisition of the late arterial phase in gemstone scintillator detector gemstone spectral imaging (GSI) mode, two to three simple mouse clicks can give subtracted iodine-only images, which improve the visualization of arterial enhancing lesions in a background nodular liver.

Another prospective advantage of this technique has been reported in posttreatment analysis of HCC, when treated with molecular targeted drug therapy, which reduces the angiogenesis within the tumor, while not causing a significant change in the size of the lesion. Quantification of tissue iodine on the iodine density images can serve as an image biomarker of tumor viability in these cases.[20,21]

## Multiphasic MR Imaging of the Liver

Over the past decades, a higher magnetic field strength and multichannel coil arrays have enabled faster MRI scanning and improved image quality. Besides, there is development of newer sequences such as MRI-PDFF (magnetic resonance imaging–proton density fat fraction) with multi-echo chemical-shift-encoded sequence for fat quantification,[22] multi-echo gradient-echo sequence for quantification of iron overload, and MR elastography (MRE) for evaluation of liver fibrosis and cirrhosis.[23] This has led to recognition of MRI as a robust and comprehensive clinical tool in liver imaging.

The protocol for multiphasic MRI of the liver (followed at our institute) is as described in ►**Table 7**.

In addition, for MRE, a modified 2D phase-contrast gradient recalled echo (GRE) pulse sequence is used to obtain four axial images from the largest transverse dimension of the liver.

An important difference between 1.5- and 3-T MRI is the capacity of acquiring high-quality thin-section postgadolinium T1-weighted 3D gradient-echo sequences on 3 T, most clinically relevant for the detection and characterization of small hypervascular malignant diseases.

### Utility of Hepatobiliary Contrast Agents

Hepatobiliary contrast agents carry the dual properties of acting like blood pool gadolinium-based contrast agents during the first pass and early phases of contrast enhancement, followed by the characteristic delayed or hepatobiliary enhancement (►**Fig. 7**). In the initial phases after injection, their contrast enhancement is dominated by the distribution in vessels and the extracellular space, like in conventional gadolinium-based contrast agents. However, unlike other contrast agents, these contrast agents are then taken up by functional hepatocytes. As a result, there is a persistent enhancement in hepatocytes that allows for identifying lesions of hepatocellular origin.

In addition, biliary excretion of this contrast allows for both identifying lesions that contain biliary canaliculi and enhancing the biliary excretion system.[24] Lesion de-enhancement described in the hepatobiliary phase of MRI is one of the ancillary features, favoring malignancy in LI-RADS documentation.[2]

Gadobenate dimeglumine and gadoxetate disodium are the commercially available hepatobiliary contrast agents. Whereas 5% of gadobenate dimeglumine is taken up by the liver, gadoxetate disodium is more hepatospecific and ~50% of this contrast is excreted through the hepatobiliary system. However, the latter is available only in Europe (commercially known as Primovist) and in United States (commercially known as Eovist). Delayed hepatobiliary phase with gadoxetate is obtained 20 minutes postcontrast injection, whereas with gadobenate, the hepatobiliary phase is obtained at 45 to 60 minutes.

Several studies have shown that MRI with a hepatobiliary contrast material is more sensitive than MRI with an extracellular contrast material in the detection of HCC, probably because MRI with a hepatobiliary contrast material displays "hepatobiliary phase (HBP) hypointense nodules without arterial phase hyperenhancement (APHE)," which often progress to HCC.[25,26]

**Table 7** Multiphasic liver magnetic resonance imaging (MRI) on 3-T scanner: protocol

| Magnetic strength | 3-T, 60-cm bore, closed scanner |
|---|---|
| Type of magnet | Superconducting |
| Line of sight/FOV | 48 cm |
| Gradient slew rate | 200 mT/m/μs |
| Coil | 32-channel body phased-array coil |
| Sequences | Axial and coronal T2-weighted sequence |
| | Axial and coronal fat-suppressed fast spin echo T2-weighted sequence |
| | Axial diffusion weighted sequence (*B*-values of –50, 500, and 800) |
| | Axial 3D T1-weighted dual echo sequence (breath hold) |
| | IDEAL-IQ (Iterative Decomposition of water and fat with Echo Asymmetry and Least squares estimation) 3D sequence for mapping of fat and iron (breath hold) |
| | Precontrast 3D T1-wieghted gradient echo breath hold sequence |
| Contrast medium | Gadobenate dimeglumine |
| Dose of contrast | 15 mL |
| Rate of contrast injection | 2 mL/s |
| Postcontrast sequences | 5 postcontrast phases with 10-s delay between each of the phases with 3D T1-weighted gradient echo breath hold sequences |
| | Delayed scans at 1, 5, and 45 min |

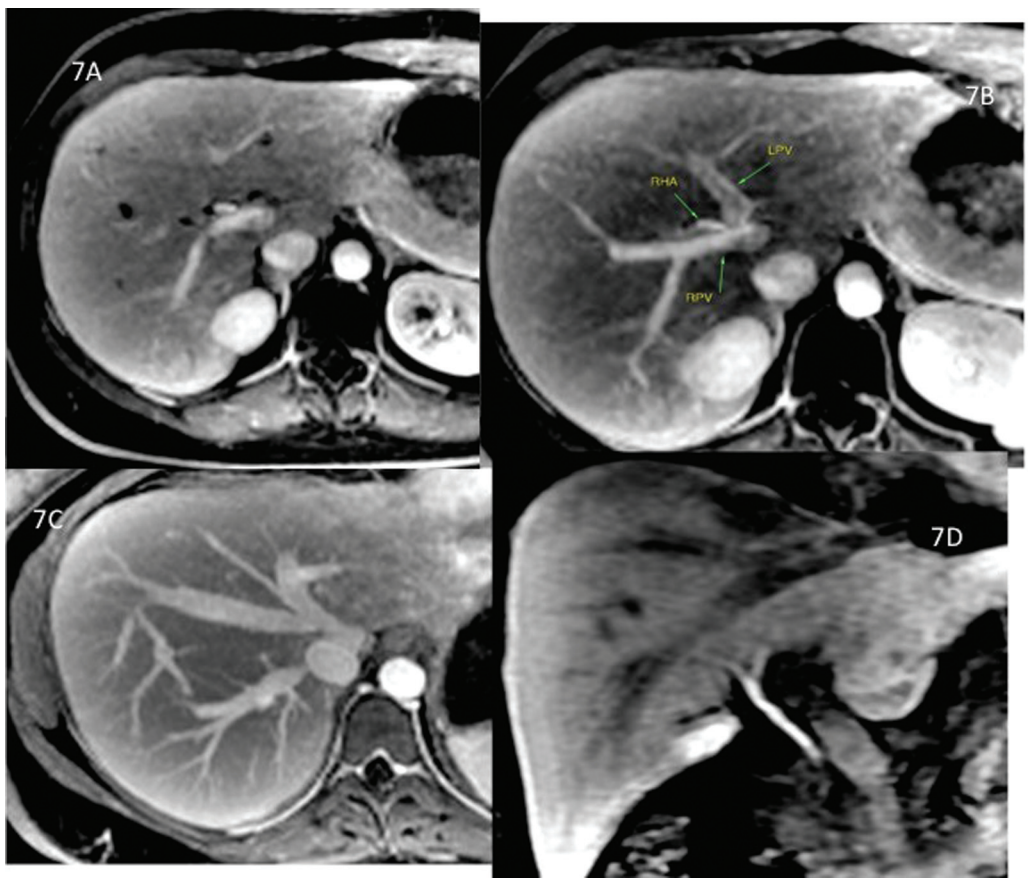


**Fig. 7** Magnetic resonance (MR) images of liver: postcontrast early arterial, late arterial, venous, and hepatobiliary phases.

### Magnetic Resonance Elastography

This MRI technique quantitatively evaluates tissue stiffness by propagating low-frequency mechanical waves through the liver. It is performed using an MRI safe passive driver that is applied to the right upper abdomen and lower chest overlying the right lobe of the liver while the patient is being

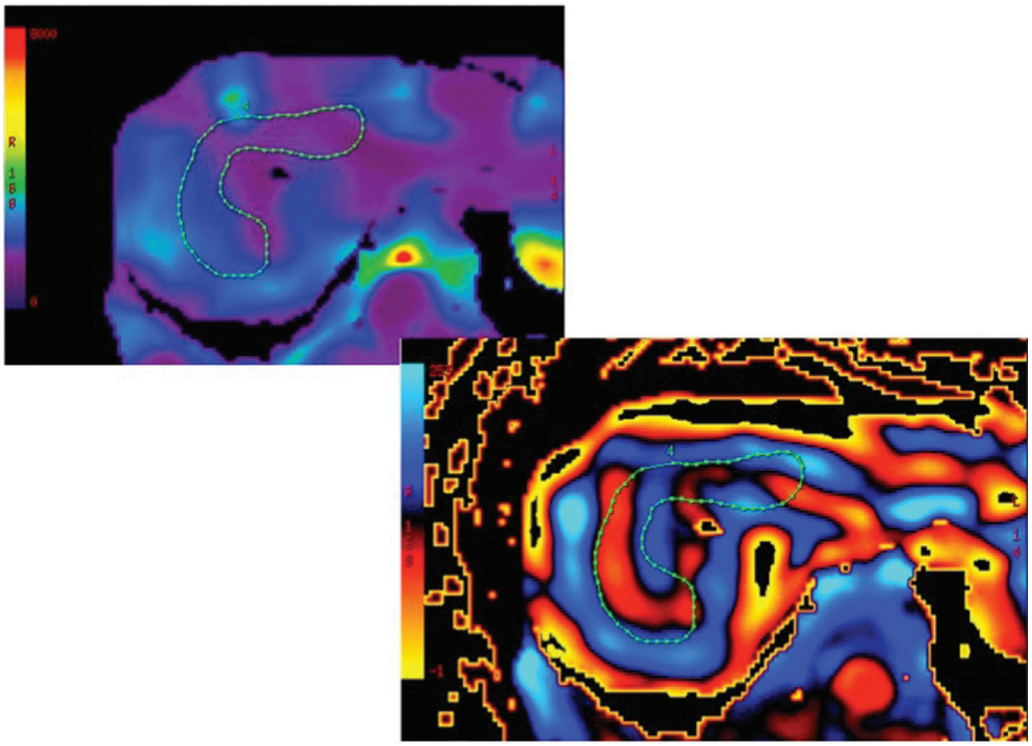

**Fig. 8** Magnetic resonance (MR) elastography color map depicting stiffness score of the liver.

scanned in the MRI scanner. The MRE sequence is performed with four short breath holds and completed within 1 to 2 minutes, without the need for intravenous contrast injection.[27]

An active driver generates low-frequency mechanical waves (typically at 60 Hz), which are conducted to the passive driver through a long plastic tube. The passive driver vibrates and produces shear waves that are propagated across the liver. The wavelength of the propagating shear wave is directly proportional to the stiffness of the liver, that is, the stiffer the liver, the longer the wavelength.

By applying an inversion algorithm to the raw data, elastograms or stiffness maps that depict tissue stiffness are generated. Elastograms may be displayed in grayscale or color scale. The result is obtained by placing the region of interest (ROI) on the processed images (►**Fig. 8**). It is measured in kilopascals (kPa). Hence, this technique requires an additional investment in elastography-specific hardware

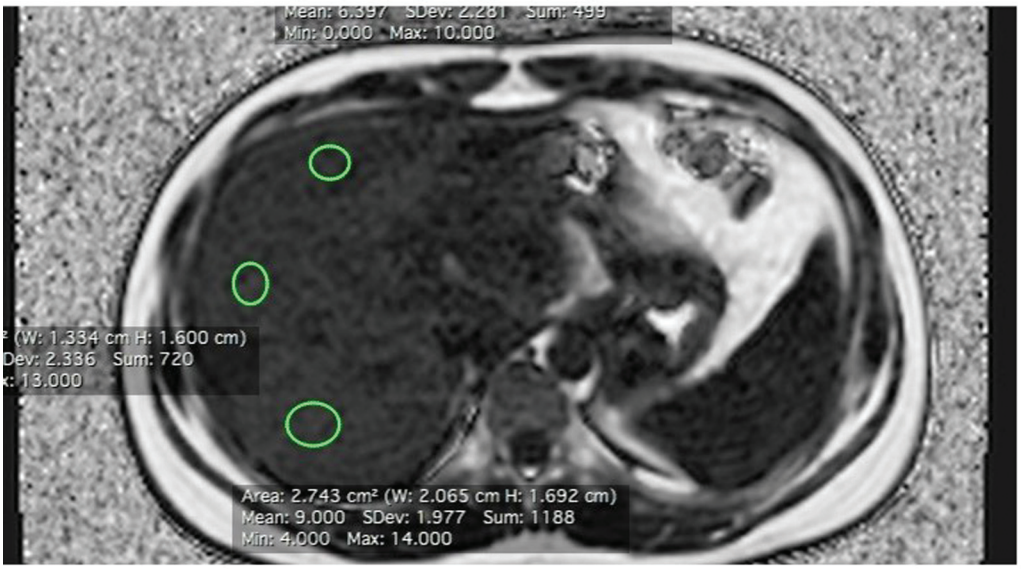


**Fig. 9** Axial section of magnetic resonance (MR) of the liver: fat fraction quantification.

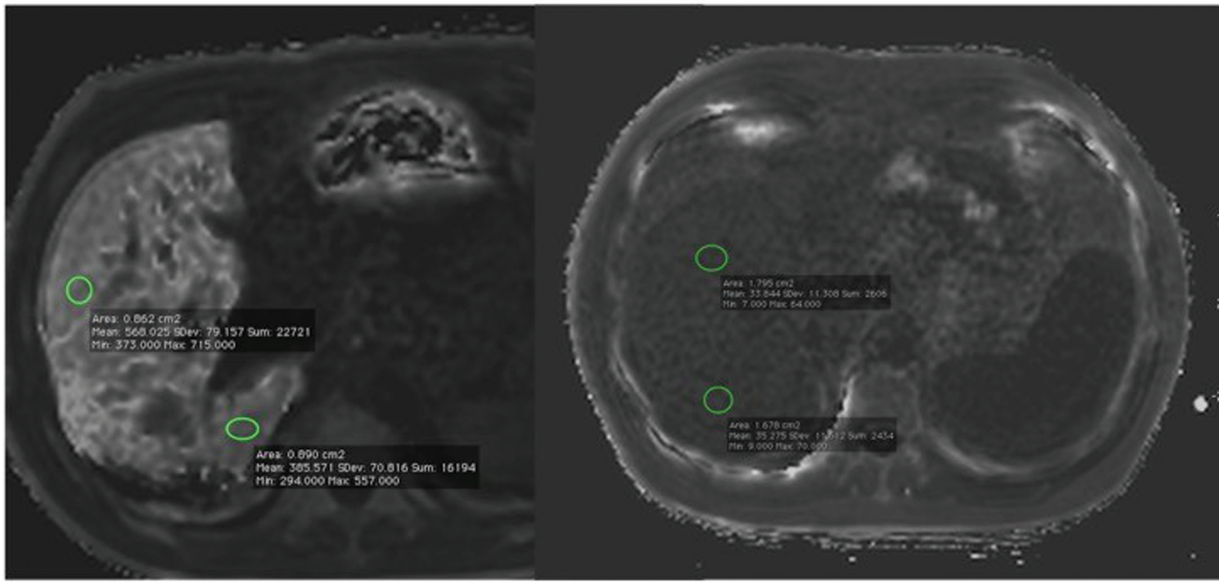


**Fig. 10** Magnetic resonance (MR) iron quantification: R2* relaxometry.

and software, with the MRI scanner, limiting its availability to centers dedicated to hepatobiliary surgery and liver transplantation.

### MRI Quantification of Fat Content of Liver

MR is sensitive to signal from protons in mobile water and triglycerides. The difference in resonant frequency of these different molecules forms the basis of chemical shift imaging, and can quantify the differential amounts of fat and water in tissues. This technique is the basic principle for PDFF technique.

PDFF is defined as the ratio of the density of mobile protons from triglycerides and the total density of protons from mobile triglycerides and mobile water. It is expressed as an absolute percentage and ranges from 0 to 100%. This technique is well correlated with a histological assessment of hepatic steatosis, which is expressed as the percentage of cells containing intracellular droplets of fat.[28] It is a single breath hold technique (~15–20 seconds) and results are in the form of images, in which the ROI can be placed on the liver and the value thus obtained equates fat content in percentage (as shown in ►**Fig. 9**).

### MR Quantification of Iron Content of the Liver

T2 represents the time constant of the intrinsic decay of the transverse magnetization from spin–spin interactions, while T2* also incorporates effects from local magnetic field inhomogeneities. The superparamagnetic effect of ferritin and hemosiderin creates a local susceptibility-induced contribution to the local magnetic field that results in faster decay of the transverse magnetization. This decay and hence iron content can be detected and quantified using GRE sequences due to their increased sensitivity to magnetic susceptibility. Recent techniques for iron quantification in clinical practice are with the use of single breath hold multi-echo gradient sequence, whereby the R2* values of the liver and in turn T2* (1/R2*) values can be obtained (►**Fig. 10**).

In multiple studies, R2* has been demonstrated to have a linear correlation with biopsy-determined liver iron content, which makes R2* relaxometry a reliable technique for non-invasive liver iron overload quantification.[29]

## Conclusion

Thorough knowledge of liver anatomy and optimal cross-sectional imaging techniques is essential for proper interpretation of liver pathologies and to provide effective guidance in patient treatment and care.

Conflict of Interest
None declared.

### References

1 Chernyak V, Fowler KJ, Kamaya A, et al. Liver Imaging Reporting and Data System (LI-RADS) version 2018: imaging of hepatocellular carcinoma in at-risk patients. Radiology 2018;289(03): 816–830
2 Couinaud C. Le foie: études anatomiques et chirurgicales. Paris: Masson; 1957
3 Strasberg SM, Belghiti J, Clavien PA, et al. The Brisbane 2000 terminology of liver anatomy and resections. HPB (Oxford) 2000; 2(03):333–339
4 Auh YH, Rosen A, Rubenstein WA, Engel IA, Whalen JP, Kazam E. CT of the papillary process of the caudate lobe of the liver. AJR Am J Roentgenol 1984;142(03):535–538
5 Noussios G, Dimitriou I, Chatzis I, Katsourakis A. The main anatomic variations of the hepatic artery and their importance in surgical practice: review of the literature. J Clin Med Res 2017;9 (04):248–252
6 Gurgacz AM, Horbaczewska A, Klimek-Piotrowska W, Walocha J. Variations in hepatic vascularisation: lack of a proper hepatic artery. Two case reports. Folia Morphol (Warsz) 2011;70(02): 130–134
7 Koç Z, Oğuzkurt L, Ulusan S. Portal vein variations: clinical implications and frequencies in routine abdominal multidetector CT. Diagn Interv Radiol 2007;13(02):75–80

8 Atasoy C, Ozyürek E. Prevalence and types of main and right portal vein branching variations on MDCT. AJR Am J Roentgenol 2006; 187(03):676–681

9 Germain T, Favelier S, Cercueil JP, Denys A, Krausé D, Guiu B. Liver segmentation: practical tips. Diagn Interv Imaging 2014;95(11): 1003–1016

10 Sahani D, Mehta A, Blake M, Prasad S, Harris G, Saini S. Preoperative hepatic vascular evaluation with CT and MR angiography: implications for surgery. Radiographics 2004;24(05): 1367–1380

11 Soyer P, Bluemke DA, Choti MA, Fishman EK. Variations in the intrahepatic portions of the hepatic and portal veins: findings on helical CT scans during arterial portography. AJR Am J Roentgenol 1995;164(01):103–108

12 Soyer P, Heath D, Bluemke DA, et al. Three-dimensional helical CT of intrahepatic venous structures: comparison of three rendering techniques. J Comput Assist Tomogr 1996;20(01):122–127

13 Koc Z, Ulusan S, Oguzkurt L, Tokmak N. Venous variants and anomalies on routine abdominal multi-detector row CT. Eur J Radiol 2007;61(02):267–278

14 Castaing D. Surgical anatomy of the biliary tract. HPB (Oxford) 2008;10(02):72–76

15 Huang TL, Cheng YF, Chen CL, Chen TY, Lee TY. Variants of the bile ducts: clinical application in the potential donor of living-related hepatic transplantation. Transplant Proc 1996;28(03): 1669–1670

16 Wald C, Russo MW, Heimbach JK, Hussain HK, Pomfret EA, Bruix J. New OPTN/UNOS policy for liver transplant allocation: standardization of liver imaging, diagnosis, classification, and reporting of hepatocellular carcinoma. Radiology 2013;266(02):376–382

17 Sultana S, Awai K, Nakayama Y, et al. Hypervascular hepatocellular carcinomas: bolus tracking with a 40-detector CT scanner to time arterial phase imaging. Radiology 2007;243(01):140–147

18 Ikram NS, Yee J, Weinstein S, et al. Multiple arterial phase MRI of arterial hypervascular hepatic lesions: improved arterial phase capture and lesion enhancement. Abdom Radiol (NY) 2017;42 (03):870–876

19 Vernuccio F, Marin D. CT material identification. In: Samei E, Pelc N, eds. Computed Tomography. Cham: Springer; 2020:305–318

20 Heye T, Nelson RC, Ho LM, Marin D, Boll DT. Dual-energy CT applications in the abdomen. AJR Am J Roentgenol 2012;199(5, Suppl):S64–S70

21 Lee SH, Lee JM, Kim KW, et al. Dual-energy computed tomography to assess tumor response to hepatic radiofrequency ablation: potential diagnostic value of virtual noncontrast images and iodine maps. Invest Radiol 2011;46(02):77–84

22 Gu J, Liu S, Du S, et al. Diagnostic value of MRI-PDFF for hepatic steatosis in patients with non-alcoholic fatty liver disease: a meta-analysis. Eur Radiol 2019;29(07):3564–3573

23 Venkatesh SK, Yin M, Ehman RL. Magnetic resonance elastography of liver: technique, analysis, and clinical applications. J Magn Reson Imaging 2013;37(03):544–555

24 Frydrychowicz A. Review of hepatobiliary contrast agents: current applications and challenges. Clin Liver Dis (Hoboken) 2018; 11(01):22–26

25 Hyodo T, Murakami T, Imai Y, et al. Hypovascular nodules in patients with chronic liver disease: risk factors for development of hypervascular hepatocellular carcinoma. Radiology 2013;266 (02):480–490

26 Ahn SS, Kim MJ, Lim JS, Hong HS, Chung YE, Choi JY. Added value of gadoxetic acid-enhanced hepatobiliary phase MR imaging in the diagnosis of hepatocellular carcinoma. Radiology 2010;255(02): 459–466

27 Guglielmo FF, Venkatesh SK, Mitchell DG. Liver MR elastography technique and image interpretation: pearls and pitfalls. Radiographics 2019;39(07):1983–2002

28 Kleiner DE, Brunt EM, Van Natta M, et al; Nonalcoholic Steatohepatitis Clinical Research Network. Design and validation of a histological scoring system for nonalcoholic fatty liver disease. Hepatology 2005;41(06):1313–1321

29 Wood JC, Enriquez C, Ghugre N, et al. MRI R2 and R2* mapping accurately estimates hepatic iron concentration in transfusion-dependent thalassemia and sickle cell disease patients. Blood 2005;106(04):1460–1465